

the ratios of the intensities of $K\alpha 1$ and $K\alpha 2$ lines and their energies $E_{K\alpha 1}$ and $E_{K\alpha 2}$, all of which are available in the literature,⁸ and

$$E_{K\alpha} = \frac{E_{K\alpha 1} + \frac{K_{\alpha 2}}{K_{\alpha 1}} E_{K\alpha 2}}{\left(1 + \frac{K_{\alpha 2}}{K_{\alpha 1}}\right)}. \quad (6)$$

From Table I it is clear that the $E_{K\alpha}$ values obtained from the present experiment are in fair agreement with those calculated using standard values for the energies of the $K\alpha 1$ and $K\alpha 2$ lines. The small deviations of about 5% or less that occur between the two $E_{K\alpha}$ values for Ta, Au, and Pb may be attributed mainly to the deviations of about 3% of the measured values of $E_{K\alpha\beta}$ from the values computed using standard literature values. These deviations are due to the poor resolution of the NaI(Tl) detector and also to uncertainties associated with the $K\beta/K\alpha$ ratios at higher Z values. We see in Table I, that the values of $(E_{K\alpha})_{\text{der}}$ are in fair agreement with the literature values and with the values calculated using Eqs. (2) and (3), although small deviations, especially at higher Z values, are clearly present. These deviations may be attributed to the fact that Bohr's frequency condition corresponds to a single-electron atom and Moseley's modification of Z to $(Z-1)$ is only an approximate way of treating screening in a multielectron atom. Taking these facts into consideration, we can say that the observed values agree fairly well with those calculated using Eqs. (2) and (3). Thus, Bohr's frequency condition and Moseley's law are verified experimentally.

We can display the results graphically and determine R , the Rydberg constant, from the present experiment. In Fig. 4, we plot $\log_{10}(E_{K\alpha})_{\text{der}}$ as a function of $\log_{10}(Z)$. From Fig. 4 we see that the data fall along a straight line with a slope of 2.1, in good agreement with the value 2 expected from Eq. (2). In Fig. 5, we present a Moseley plot for elements in the atomic number range from $Z=42$ to $Z=82$. We see, in Fig.

5, that there is a linear dependence between $(E_{K\alpha})_{\text{der}}$ and $(Z-1)^2$, and from the slope we obtain an experimental value for the Rydberg constant, $R = (1.19 \pm 0.01) \times 10^7 \text{ m}^{-1}$, in fair agreement with the literature value⁹ $10\,973\,731.534(13) \text{ m}^{-1}$ for an infinitely heavy nucleus.

Moseley's law indicates that as one goes from the lighter elements to the heavier elements, the energy of the characteristic x rays emitted from a sample increases in a regular manner and is approximately proportional to $(Z-1)^2$, from which the atomic number Z of a sample can be identified. That is how Moseley was able to identify, from his investigations, the place of Co and Ni, whose atomic weights are in reverse order in the periodic chart.

ACKNOWLEDGMENT

One of the authors (S.B.G.) would like to thank the Karnataka University Dharwad, for the Research Fellowship.

^aElectronic mail: nagappa123@yahoo.co.in

^bPresent address: Vice-Chancellor, Mangalore University, Mangalagangotri-574199, Karnataka, India.

¹C. Hohenemser and I. M. Asher, "A simple apparatus for Moseley's law," *Am. J. Phys.* **36** (10), 882–885 (1968).

²Arthur M. Lesk, "Reinterpretation of Moseley's experiments relating $K\alpha$ line frequencies and atomic number," *Am. J. Phys.* **48** (6), 492–494 (1980).

³P. J. Ouseph and K. H. Hoskins, "Moseley's law," *Am. J. Phys.* **50** (3), 276–277 (1982).

⁴C. W. Haigh, "Moseley's work on x-rays and atomic number," *Am. J. Phys.* **72** (11), 1012–1014 (1995).

⁵C. W. S. Conover and John Dudek, "An undergraduate experiment on x-ray spectra and Moseley's law using a scanning electron microscope," *Am. J. Phys.* **64** (3), 335–338 (1996).

⁶Robley D. Evans, *The Atomic Nucleus* (Tata-McGraw-Hill, Bombay-New Delhi, 1955), pp. 21–22.

⁷James H. Scofield, "Relativistic Hartree–Slater values for K and L x-ray emission rates," *At. Data Nucl. Data Tables* **14**, 121–137 (1974).

⁸N. A. Dyson, *X-rays in Atomic and Nuclear Physics* (Cambridge U.P., Cambridge, 1990), 2nd ed., pp. 378–384.

⁹E. Richard Cohen and Barry N. Taylor, "The 1986 adjustment of the fundamental physical constants," *Rev. Mod. Phys.* **59** (4), 1121–1148 (1987).

A simple vibrating sample magnetometer for use in a materials physics course

Wesley Burgei,^a Michael J. Pechan, and Herbert Jaeger
Department of Physics, Miami University, Oxford, Ohio 45056

(Received 24 June 2002; accepted 14 March 2003)

An inexpensive vibrating sample magnetometer (VSM) has been developed for use in a materials physics course. An exercise using the VSM allows students to measure the magnetic properties of various materials and thus gain experience applicable to contemporary research on magnetic materials. This paper describes specific aspects of the construction of a VSM and presents measurements for two 5-mm-long Ni wires of different diameters and for floppy disk media. A 178- μm -diam Ni wire served as a calibration sample for the system; the results from a 51- μm -diam Ni wire set the limit of precision for this system at approximately 5×10^{-3} emu. © 2003 American Association of Physics Teachers.

[DOI: 10.1119/1.1572149]

I. INTRODUCTION

The vibrating sample magnetometer (VSM), pioneered by S. Foner,¹ is a simple yet effective technique for characteriz-

ing properties of magnetic materials. Due to its straightforward design and continued use among condensed matter physicists and materials scientists, the VSM provides an ideal laboratory exercise for students in an advanced materi-

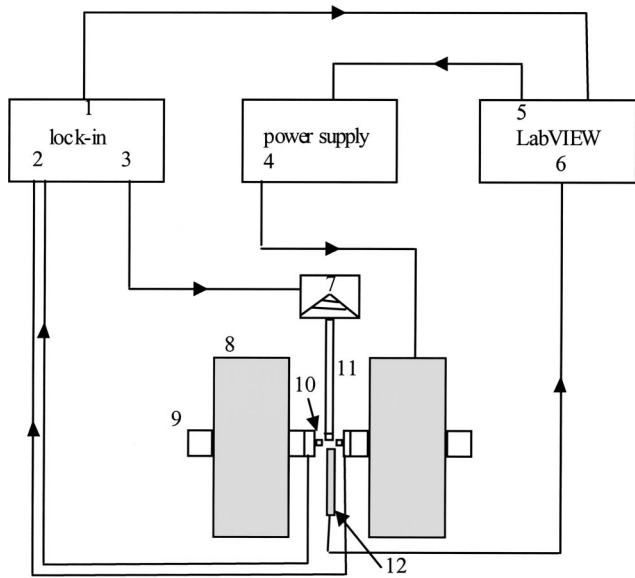


Fig. 1. Schematic diagram of the VSM apparatus showing: (1) coil measurement signal path from the lock-in to LabVIEW via GPIB, (2) signal from the detection coils, (3) driving signal from the lock-in to the mechanical vibrator, (4) the power supply connection to the magnet, (5) the power supply control signal from LabVIEW, (6) the Hall-probe input to LabVIEW via the DAC, (7) mechanical vibrator, (8) electromagnet, (9) magnet pole pieces, (10) detection coil, (11) drinking straw shaft, and (12) Hall probe.

als physics course. This setup allows exploration of a common experimental technique for measuring magnetic material properties such as hysteresis, saturation, coercivity, and anisotropy. The VSM is one of a number of techniques illustrated in our materials physics laboratory course² that emphasizes measurement and characterization of various materials.

Based on Faraday's law of induction, the VSM relies on the detection of the emf induced in a coil of wire given by

$$\varepsilon = -N \frac{d}{dt}(BA \cos \vartheta), \quad (1)$$

where N is the number of wire turns in the coil, A is the coil turn area, and ϑ is the angle between the B field and the direction normal to the coil surface. In practice, knowledge of coil parameters such as N and A is unnecessary if the system can be calibrated with a known sample.

The operation of the VSM is fairly simple. A magnetic sample is placed on a long rod and then driven by a mechanical vibrator. The rod is positioned between the pole pieces of an electromagnet, to which detection coils have been mounted. The oscillatory motion of the magnetized sample will induce a voltage in the detection coils. The induced voltage is proportional to the sample's magnetization, which can be varied by changing the dc magnetic field produced by the electromagnet.

This article focuses on the construction and operation of a relatively inexpensive VSM for a materials physics course. The construction could also serve as a student project. Other than a commercial lock-in amplifier, a variable dc power supply, and a small electromagnet, only inexpensive and readily available components are required for implementation in a teaching laboratory.

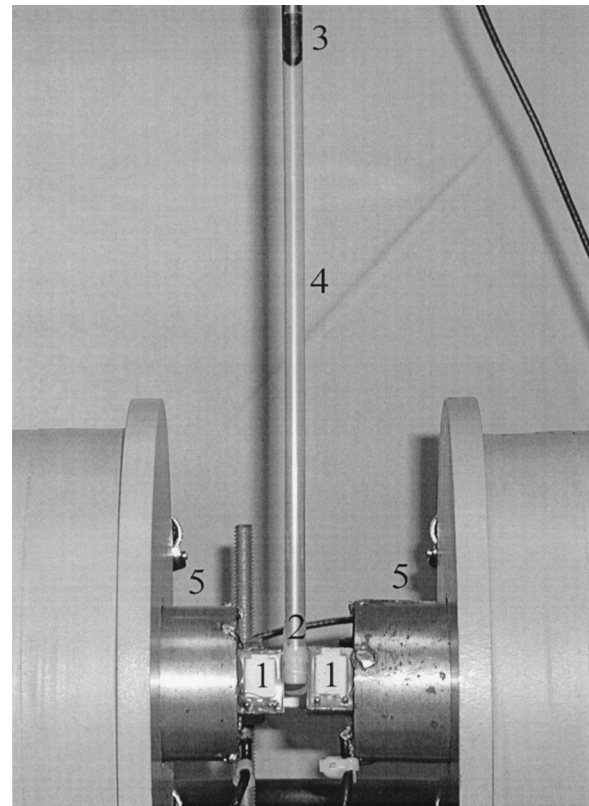


Fig. 2. Photograph of the VSM showing: (1) sense coils, (2) acetal sample mount covered in parafilm, (3) banana plug connector, (4) soda straw sample rod, and (5) magnet pole pieces. The solenoid axis of each sense coil is oriented parallel to the sample rod.

II. APPARATUS

The layout of our VSM is depicted schematically in Fig. 1, and a photograph of the sample rod and pickup coil area is shown in Fig. 2.

A. Oscillating sample mount

Sample oscillation is provided by a Pasco Scientific Model SF-9324 mechanical drive that is mounted to an $x-y-z$ translator³ so that the sample can be centered easily between the magnet poles. The shaft of the sample mount is a long clear drinking straw, which is tightly fitted to the bottom of the mechanical vibrator by a banana plug. We have found that for the intended purposes, the drinking straw provides enough strength and rigidity; however, one could also use a mechanical guide to prevent excess nonaxial motion. An acetal cylinder was machined and fitted inside the bottom of the drinking straw to provide a sample mount. The sample can be fastened with either vacuum grease or a small piece of *Parafilm*[®], the latter being used in our case since the small pole pieces and wide gap produced significant field gradients tending to dislodge the sample. To correct for small variations in vibration amplitude and frequency with time, a reference coil and magnet are often used in research-grade investigations, but they are not employed in the present apparatus.

B. Experimental magnetic field

An air-cooled *GMW*[®] Model 3470 electromagnet with 45-mm-diam pole pieces provides the external applied field. The

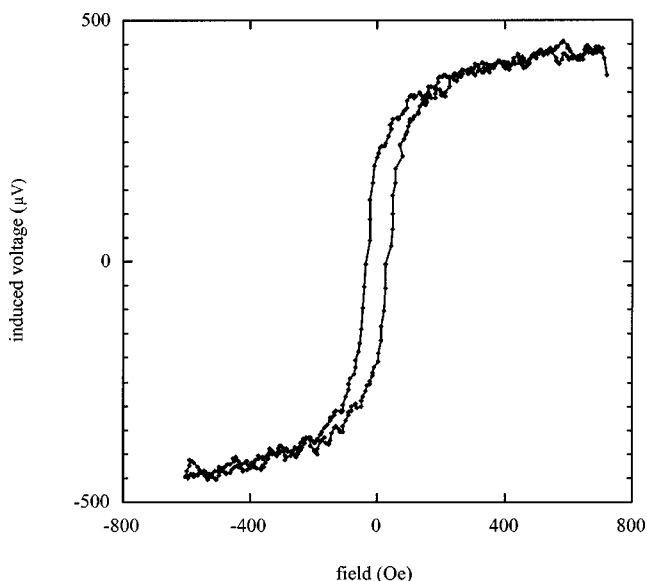


Fig. 3. Hysteresis loop for a Ni wire sample of 5-mm length and 178- μm diameter. This sample is used for magnetization calibration. [To convert to SI units, use 1 oersted (Oe) = $(10^3/4\pi)$ (A/m)].

magnet is powered by a voltage-controlled *Kepeco*[®] 36V/6A bipolar power supply. The magnetic field is measured by an *F.W. Bell*[®] Model 5080 Gauss-meter with analog output capabilities; its Hall probe is mounted between the magnet pole pieces close to the sample position. The electromagnet is attached to a rotating base, which consists of a lazy-susan-type ball bearing rotator and a circular wooden base. This feature allows measurements to be made as a function of angle. As mentioned above, the combination of the small pole-piece diameter and the wide gap necessary to accommodate the detection coils yields a significant magnetic field gradient in the sample region. The field gradient adds noise to the system by introducing a force on the sample that creates nonaxial motion of the straw shaft.

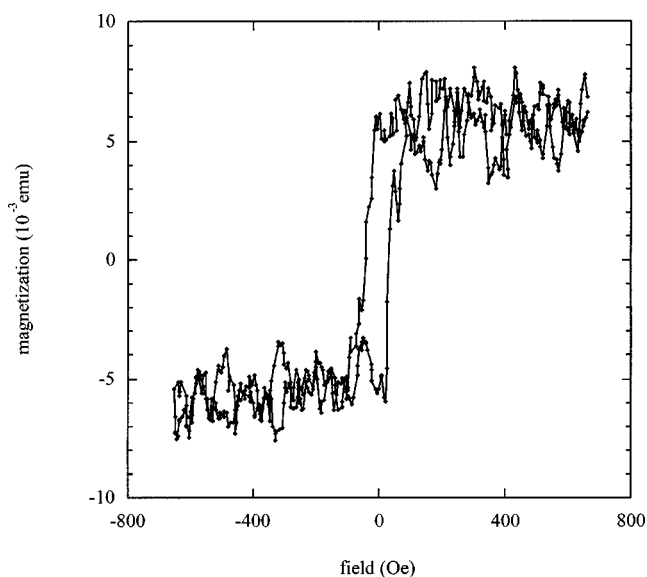


Fig. 4. Hysteresis loop for a Ni wire sample of 5-mm length and 51- μm diameter. This measurement demonstrates the lower level of precision for this system.

C. Signal detection

The most important component that determines the system's resolution is the pick-up coil assembly. While commercial pick-up coils would, of course, provide the highest sensitivity, satisfactory results can be obtained using coils extracted from electro-mechanical relays. In our case, two 32k coils were removed from electromechanical relays;⁴ each coil had an axial length of 18 mm and outer radius of approximately 12 mm. The iron cores of the coils were left in place to increase sensitivity. Each coil was attached with mounting wax to a printed circuit board that was etched with pads for the coil leads and for the coaxial cable running to the lock-in amplifier. The printed circuit board was then attached to the magnet pole pieces so that the cylindrical axis of each pick-up coil was collinear to and coplanar with the axis of sample vibration. The coils are wired so that their induced emfs sum.

Since we are measuring an ac signal and desire to optimize signal-to-noise, we use synchronous detection. We use a *Stanford Research Systems* Model SR830 lock-in amplifier, which is set to lock-on to a signal oscillating at the driving frequency. We use the lock-in amplifier to provide a signal that drives the mechanical vibrator and also serves as the reference signal for the lock-in; however, one could just as easily use a separate function generator for the driving signal and provide it to the lock-in amplifier as a reference signal. It should be noted that if a commercial lock-in amplifier is not available, a less flexible substitute may be constructed using an Analog Devices AD630 balanced mod/demod IC and Burr-Brown's 4423 quadrature oscillator.⁵

D. Automated data collection

A LabVIEW[™] program provides experimental control and data acquisition. The program produces a calibrated analog signal, through a National Instruments Model 6024A data acquisition card (DAQ), which sets the current of the power supply so as to provide the desired magnetic field. The program then sweeps the field from high to low, and then back to high, in steps determined by the user. At each field setting, the induced signal read by the lock-in amplifier is transferred to the computer through the GPIB bus, and the output of the Hall probe is measured through the DAQ. Once the program completes a field cycle, the data are plotted and saved to a text file. All measurements could just as well be made using the DAQ card and analog outputs from the instruments.

III. RESULTS

In our materials physics course, three samples are used to illustrate the VSM technique. Figure 3 shows data from a 5-mm length of 178- μm -diam Ni wire⁶ used for signal calibration. An external field, applied parallel to the sample length, is swept through a complete cycle in order to record a hysteresis loop. Then, using the known Ni magnetization,⁷ 500 emu/cm³, and the known wire volume, we can convert the high field voltage signal (where the magnetization is saturated) into emu units.⁸ (To convert to SI units, use 1 emu/cm³ = 10³ A/m.) Figure 4 shows data from a 5-mm length of 51- μm -diam Ni wire (also with its length parallel to the applied field) that demonstrates the lower limit of resolution of this system is about 5×10^{-3} emu with a signal-to-noise ratio of 3:1. Despite the low signal-to-noise ratio, the magnetic moment of this sample is consistent with that of the

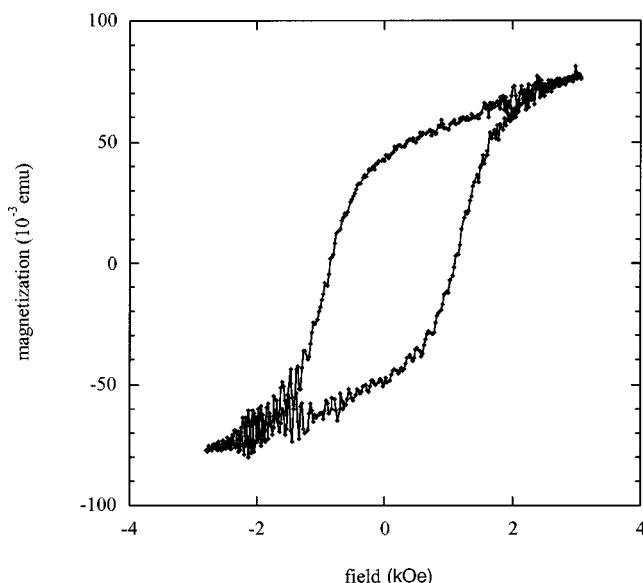


Fig. 5. Hysteresis loop for 5-mm-diameter circular pieces of floppy disk material. Five pieces were stacked together.

178- μm Ni wire if the difference in volume of the two wires is taken into account. Both Ni wire samples exhibit approximately the same coercive field, which is defined as the field producing zero magnetization upon reversal. However, the remnant field—the magnetization in zero field—is quite different for the two. The 51- μm -diam Ni wire is characterized by a square loop with high remnance, implying it has a very abrupt magnetization reversal, whereas the 178- μm sample has lower remnance, consistent with a more gradual reversal process. These results are consistent with shape anisotropy arising from demagnetization effects in a rod-like sample.⁹ Since the length-to-diameter aspect ratio is 3.5 times greater for the 51- μm wire, the shape anisotropy is much greater and therefore more effective in keeping the magnetization along the long axis of the wire. This anisotropy is competing with the randomly oriented crystalline anisotropies associated with the polycrystalline nature of the wire. In the thin wire, the shape anisotropy dominates, whereas in the thick wire, the effect of the randomly oriented crystallites is more evident.

The third sample examined is floppy disk material cut using a hole-punch to make circular pieces with a diameter of 5 mm. Five pieces were stacked together and measurements made with the magnetic field parallel to the planes of the disks. This stack provides a large signal with a good signal-to-noise ratio, as seen in Fig. 5. The resulting hysteresis loop is wide with a relatively high coercivity that is typical of magnetic storage materials. The oscillatory noise at higher fields is due to transverse motion of the sample rod induced by the field gradient.

One could easily investigate the magnetic properties of other readily available samples such as small pieces of paper clip or iron filings.

IV. SUMMARY

The construction and operation of an inexpensive VSM for a materials physics course has been described in detail. Ni wire and floppy disk samples were examined, and, with a magnetization resolution of about 5×10^{-3} emu, this simple VSM provided results that illustrated basic properties of magnetic materials and were suitable for quantitative analysis.

^aElectronic mail: burgeiwa@muohio.edu

¹S. Foner, "Versatile and Sensitive Vibrating-Sample Magnetometer," *Rev. Sci. Instrum.* **30** (7), 548–557 (1959).

²H. Jaeger, M. J. Pechan, and D. K. Lottis, "Materials physics: A new contemporary undergraduate laboratory," *Am. J. Phys.* **66** (8), 724–730 (1998).

³Parts 5200 and 1185, Sherline Products, Inc., 3235 Executive Ridge, Vista, CA 92083-8527.

⁴Part #RTB14730, Schrack Energietechnik GmbH, Seybelgasse 13, 1235 Wien, Austria.

⁵M. J. Pechan, J. Xu, and L. D. Johnson, "Automatic frequency control for solid-state sources in electron spin resonance," *Rev. Sci. Instrum.* **63** (7), 3666 (1992).

⁶California Fine Wire Company, 338 So. Fourth Street, Grover Beach, CA 93433-0199.

⁷Charles Kittel, *Introduction to Solid State Physics* (Wiley, New York, 1986), 6th ed., p. 429.

⁸B. D. Cullity, *Introduction to Magnetic Materials* (Addison-Wesley, Reading, MA, 1972), p. 7.

⁹Reference 8, p. 240.